

NASA TECHNICAL NOTE



NASA TN D-5400

2.1

NASA TN D-5400



LOAN COPY: RETURN TO
AFWL (WL0L-2)
KIRTLAND AFB, N MEX

HYDRATION, OXIDATION, AND THE ORIGIN OF THE CALC-ALKALI SERIES

by Robert F. Mueller

*Goddard Space Flight Center
Greenbelt, Md.*



HYDRATION, OXIDATION, AND THE ORIGIN
OF THE CALC-ALKALI SERIES

By Robert F. Mueller

Goddard Space Flight Center
Greenbelt, Md.

NATIONAL AERONAUTICS AND SPACE ADMINISTRATION

For sale by the Clearinghouse for Federal Scientific and Technical Information
Springfield, Virginia 22151 -- Price \$3.00

ABSTRACT

A physicochemical interpretation is given for the calc-alkali differentiation series of igneous rocks as distinguished particularly from gabbroic series such as the Skaergaard complex. It is found that, contrary to previous assumptions, the oxygen fugacity decreases markedly during calc-alkaline differentiation and in this way resembles the situation in gabbroic complexes. The affinity of water for the melt has the important consequence of increasing the solubilities of the quartzo-feldspathic components more than those of the ferromagnesian components, so that the phase boundaries are shifted toward lower liquidus temperatures. The result is that the courses of the crystallization paths are directed into a region of quartzo-feldspathic rather than gabbroic liquids.

SUMMARY

A physicochemical interpretation is given for the calc-alkali differentiation series of igneous rocks as distinguished particularly from gabbroic series such as the Skaergaard complex. It is found that, contrary to previous assumptions, the oxygen fugacity decreases markedly during calc-alkaline differentiation and in this way resembles the situation in gabbroic complexes. The principal index of this decrease is the systematic increase in the atomic fraction $\text{Fe}^{2+}/(\text{Mg} + \text{Fe}^{2+})$ of the ferromagnesian minerals in the sequence gabbro to granite, but observed oxide phases also support this conclusion.

Application of the reaction $\text{FeSiO}_3 + 1/6 \text{O}_2 \rightleftharpoons 1/3 \text{Fe}_3\text{O}_4 + \text{SiO}_2$ to the rocks of the southern California batholith shows that the oxygen fugacity P_{O_2} may decrease by as much as 10 orders of magnitude throughout the series and that this probably corresponds to a marked decrease in the activity ratio $a_{\text{H}_2\text{O}}/a_{\text{H}_2}$ of the melt.

The decrease in oxygen fugacity with differentiation as implied by the mineral assemblages is ascribed to the tendency for H_2O to react more strongly with the silicate melt than does H_2 , so that the activity ratio of the melt systematically decreases. This same affinity of water for the melt has the even more important consequence of increasing the solubilities of the quartzo-feldspathic components more than those of the ferromagnesian components, so that the phase boundaries are shifted toward lower liquidus temperatures. The result is that the courses of the crystallization paths are directed into a region of quartzo-feldspathic rather than gabbroic liquids.

The possibility that the calc-alkali magmas may originate by mechanisms such as contamination or partial melting of crustal rocks is also discussed. It is, however, concluded that the physicochemical data, including both bulk chemical compositions and mineral compositional variations throughout the series, indicate that crystallization differentiation of a basaltic or basic magma is the most likely mechanism. This is shown particularly by the lack of evidence for addition of K_2O - and Al_2O_3 -rich crustal rocks to the magmas, although these rocks abound in the area. Also there is no evidence of the addition of material of diverse oxidation states such as might be expected if assimilation were widespread.

CONTENTS

Abstract	ii
Summary	iii
INTRODUCTION	1
CHARACTERISTICS OF THE CALC-ALKALI PLUTONIC AND VOLCANIC COMPLEXES	3
Southern California Batholith	3
Sierra Nevada and Idaho Batholiths	8
Other Plutonic Complexes	10
Volcanic Complexes	10
Summary of Observations	11
OXIDATION STATES OF MAGMATIC MINERALS AND MAGMAS	11
Mineral Indicators of P_{O_2}	11
Oxidation States of Silicate Melts	15
CONSEQUENCES OF THE DIFFERENTIAL SOLUBILITIES OF THE SILICATES	19
CORRELATIONS AND GENERAL CONCLUSIONS	21
ACKNOWLEDGMENTS	23
References	23

HYDRATION, OXIDATION, AND THE ORIGIN OF THE CALC-ALKALI SERIES

by

Robert F. Mueller
Goddard Space Flight Center

INTRODUCTION

Two major chemical variation trends leading from basaltic to granitic magmas have been generally recognized. The better documented of the two, as exemplified particularly by the Skaergaard complex of East Greenland (Reference 1), may be called the "gabbroic trend." It has been shown that this trend, which results in the formation of ferrogabbros and a small granite residue, is the consequence of the fractional crystallization of basaltic magma. The other, usually called the "calc-alkali trend," results in the more familiar series gabbro-diorite-tonalite-grandiorite-granite, which particularly characterizes the great Mesozoic batholiths of the western Americas, but which is also known throughout the world. The mechanism of the formation of the calc-alkali series is controversial, although the most frequent suggestion has been that it too results from the fractional crystallization of basaltic magma.

The problem of these diverse trends has been clearly recognized for at least 40 years, and it formed the subject of a spirited controversy between Fenner and Bowen—in fact, the absolute iron enrichment represented by the gabbroic complexes is sometimes referred to as the "Fenner trend." The problem was, however, most clearly stated by Bowen, Schairer, and Willems (Reference 2), who recognized that the answer must lie in identifying the physicochemical factors which determine whether the magma becomes enriched in its quartzo-feldspathic or its ferromagnesian components. They also recognized that, in conformity with then-existing physicochemical data, relative enrichment in iron, as expressed by the atomic fraction $\text{Fe}^{2+}/(\text{Mg} + \text{Fe}^{2+})$, was characteristic of both series. Unfortunately, at the time nothing was as yet known of the Skaergaard complex, which is the best example of absolute iron enrichment as advocated by Fenner (Reference 3).

The absolute iron enrichment in the gabbroic sequence is the result of the accumulation in the magma of Fe_2SiO_4 and FeSiO_3 under anhydrous and increasingly reducing conditions. As was demonstrated by Osborn (Reference 4), when little or no source of oxygen, such as water, exists, the magma behaves like an experimental system under the constraint of constant total composition of the condensed phases. Under these circumstances, only minute quantities of the condensed

system need react to decrease the oxygen significantly, and the fugacity steadily decreases as cooling and crystallization proceed. As a consequence, the iron component remains in the melt as soluble ferrous silicate and does not precipitate as Fe_3O_4 . This retention of the ferromagnesian component, which is increasingly enriched in FeO , is thus in approximately a constant ratio to the retention of the feldspathic component, which is increasingly enriched in albite. This may be seen by an examination of the successive Skaergaard liquids, as deduced by Wager and Deer (Reference 1).

The importance of the oxidation state of iron in basaltic magma was first stressed by Kennedy (Reference 5). He also believed (Reference 6) that the gabbroic trend was characterized by high and increasing values of $\text{FeO}/\text{Fe}_2\text{O}_3$, while in the calc-alkali trend the opposite was true. This idea was further pursued by Osborn (Reference 4), who concluded that the calc-alkali trend was distinguished by a constant or even increasing oxygen fugacity during differentiation and that this was a direct result of the high water contents of these magmas. This conclusion of Osborn's was reached largely by analogy with the experimental system $\text{MgO}-\text{FeO}-\text{Fe}_2\text{O}_3-\text{SiO}_2$ (Reference 7), in which an impressed constant oxygen fugacity gives rise to a differentiation trend leading to silica enrichment of the melt through precipitation of ferrite. However, Osborn made no attempt to assess the role of the quartz-feldspathic component of basaltic magma, nor did he attempt to show that high water content of a magma does indeed lead to highly oxidizing conditions. Since Osborn's study there have been several papers purporting to show that the oxygen fugacity does indeed behave as Osborn proposed. It is therefore of some importance to see whether this conclusion accords with observed features of natural assemblages.

The writer believes that the resolution of the problem of diverse differentiation trends lies in a knowledge of the details of the interaction of volatile constituents and the silicate melt. Quite obviously there is a close connection between the oxygen, hydrogen, and water fugacities and between the activities of these constituents in the melt. The first question that needs to be settled is whether these interactions lead to oxidizing or reducing conditions during differentiation. The second question concerns the effect of these volatiles on the course of differentiation itself.

The answer to the first question may be sought in the compositions of those minerals which are found in the calc-alkali series rocks and which reflect magmatic or near-magmatic conditions. These compositional data may be evaluated in terms of the energetics of certain pertinent reactions for which thermochemical data exist. The oxidation state so determined may, as a first approximation, be compared to the pure system O_2-H_2 to see how the oxygen fugacity P_{O_2} in this system changes over the pressure and temperature ranges involved. The same system may then be examined in terms of possible interactions with the melt to see what modifications these may impose.

The answer to the second question must be sought in the interactions of hydrogen and water with the melt so that the relative importance of these interactions can be assessed. To that end we make use of the available experimental data and theoretical models.

Finally, it will be necessary also to examine the evidence that the calc-alkali series is primarily the result of the differentiation of a basaltic magma rather than of some such process as contamination or fusion of crustal rocks.

CHARACTERISTICS OF THE CALC-ALKALI PLUTONIC AND VOLCANIC COMPLEXES

Southern California Batholith

Some of the best-known examples of calc-alkali series rocks are to be found in the large batholiths and volcanic provinces of western North America. However, only a few of these complexes have been studied in sufficient detail for our purposes. The southern California batholith is one of the largest of the complexes, and its northwestern end has been subject to the most thorough mineral chemistry study by Larsen and his co-workers. This part of the batholith, which was mapped in some detail by Larsen (Reference 8), appears to be predominantly of an igneous character, although it contains numerous screens of prebatholithic metasediments and metavolcanics. Toward the east, however, the metamorphics become much more abundant, and the batholith assumes a less clearly igneous character (Reference 9).

According to Larsen (Reference 8), the area studied by him consists of over 20 separate plutons ranging through the series gabbro-tonalite-granodiorite-granite. Furthermore, field studies indicate that this is also the time sequence of intrusion. In terms of the areas occupied by the various rock types, Larsen found the following distribution:

<u>Rock Type</u>	<u>Percent</u>
gabbro	7
tonalite	63
granodiorite	28
granite	2

Consequently, the average composition of the batholith in this region corresponds to tonalite.

Many of the features such as lithologic boundaries, gneissic texture, and the direction of extension of basic inclusions show parallelism to each other and to the regional features such as the trend of the coast line and major faults. The closely folded character of the prebatholithic metamorphic rocks (Reference 9) indicates intense deformation; and, although some of the intrusions appear to be postkinematic, there is evidence that regional deformation during late stages of consolidation was widespread. As noted by Hurlbut (Reference 10), this is particularly well shown by the regionally oriented basic inclusions which characterize the tonalites. In the eastern part of the batholith, this regional synkinematic picture is even more pronounced in the marked development of gneissic texture (Reference 9).

The igneous character of the western part of the batholith is attested by numerous criteria such as the following: (1) evidence of highly fluid flow in the form of heterogeneously mixed xenoliths of various kinds, (2) sharp zoning of plagioclase and analogous features in other minerals which are normally found when crystals precipitate from a melt, (3) smooth variation of the oxide abundance throughout the sequence, and (4) systematic changes in mineral composition which, as will be seen later, are compatible with igneous differentiation. This last point is of particular

interest, since these mineral compositional variations provide us with the index of change in such parameters as the oxygen fugacity.

The general character of the southern California rocks may be seen in Tables 1, 2, and 3. In these tables particular emphasis has been placed on the San Marcos gabbro, the earliest member of the sequence and the one which presumably resembles most closely the hypothetical parent magma. Outstanding features of gabbros of the San Marcos variety are the combination of very calcic plagioclase and abundant hornblendes (Table 2) and the high normative feldspar contents (Table 3) when compared with many other gabbros and basalts. Of special interest is the very anorthite-rich olivine gabbro, or troctolite (No. 1). According to Miller (Reference 11), this gabbro represents a crystallized liquid as attested by a unique mosaic texture, similar dike rocks, and other criteria. If this is true, this troctolite may be the crystalline equivalent of the parent magma. Another feature of particular interest is the very low K_2O content of the San Marcos gabbro as a whole and of the representative types (Table 1). These low K_2O contents also characterize the whole sequence of rock types ranging from gabbro to granite, as may be seen by

Table 1
Chemical Analyses of Representative Types and Average of the San
Marcos Gabbro, Southern California Batholith (Reference 8).

Index No.	1	2	5	Average Gabbro
Sample No.	SLR M354*	El 303*	SLR M334*	
SiO ₂	42.86	45.78	52.12	50.78
TiO ₂	0.18	5.13	0.33	0.77
Al ₂ O ₃	24.94	15.59	20.88	20.40
Fe ₂ O ₃	2.13	1.89	0.34	1.75
FeO	6.14	10.92	6.52	6.20
MnO	0.06	0.17	0.09	0.09
MgO	9.28	7.20	6.90	6.49
CaO	13.08	11.96	10.14	10.24
NaO	0.76	1.00	2.40	2.20
K ₂ O	0.09	0.42	0.25	0.45
H ₂ O ⁻	—	0.03	—	—
H ₂ O ⁺	0.78	0.36	0.22	0.65
P ₂ O ₅	none	tr	none	0.05
S	0.03	—	none	0.04
CO ₂	—	—	—	—
ZrO ₂	—	—	—	—
	100.33	100.45	100.19	100.11

*For rock names see Table 2.

Table 2

Modal Mineral Content and Mineral Compositions of Representative Rocks of the Southern California Batholith (Reference 8).

Index No.	1	2	3	4	5	6	7	8	9	10	11	12	13	14
Sample No.	SLR M354 (troctolite)	El 303 (hornblende gabbro)	SLR 218 (norite)	SLR 299 (hornblende gabbro)	SLR M334 (typical norite)	SLR 229B (norite)	El 230 (norite)	SLR 1016 (Bonsall Tonalite)	SLR 138 (Green Valley Tonalite)	El38-134 (Lakeview Tonalite)	SLR 2242 (Bonsall Granodiorite)	Ra 135 (Woodson Mountain Granodiorite)	El38 167 (Rubidoux Granite)	El38 265 (Rubidoux Granite)
Quartz	—	tr	1	—	tr	7	10	12	24	36	32	30	33	34
K-Feldspar	—	—	—	—	tr	—	—	—	—	2	14	21	32	36
Plagioclase	67	47	61	51	65	58	52	53	48	53	44	42	34	26
Biotite	—	—	1	1	tr	6	16	14	12	6	7	5	2	2
Hornblende	10	34	12	42	1	22	3	18	11	1	2	1	1	tr
Augite	—	5	10	5	4	3	8	—	3	—	—	1	—	—
Hypersthene	2	6	8	—	28	3	9	—	—	—	—	—	0.5	—
Olivine	18	—	—	—	—	—	—	—	—	—	—	—	—	—
Fe-Ore*	1	8	8	2	2	1	2	+	2	+	—	—	+	+
Spinel	1.5	—	—	—	—	—	—	—	—	—	—	—	—	—
Iddingsite	0.5	—	—	—	—	—	—	—	—	—	—	—	—	—
Undifferentiated Accessories	+	+	+	+	+	+	+	2	+	1	1	1	+	+
An in plag.	93	86	59	70	64	49	50	47	38	35	32	25	21	18
Fe ²⁺ orthopyroxene	—	—	—	—	0.346	—	—	—	—	—	—	—	0.768	—
Fe ²⁺ hornblende	0.231	—	—	—	—	0.372	—	0.408	0.408	0.447	0.437	0.524	0.745	—
Mg + Fe ²⁺ biotite	—	—	—	—	—	—	0.457	0.450	0.463	0.500	0.509	0.587	0.723	0.782

+Indicates that mineral is present.

*Magnetite and Fe-Ti oxides.

Table 3

Weight Norms of Rocks from the Southern California Batholith
(Larsen, 1948).

Index No.	1	2	3	4	5	6	7	
Sample No.	SLR M354	El 303	SLR 218	SLR 299	SLR M334	SLR 229B	El 230	Average San Marcos Gabbro
Q	—	2.28	1.38	—	1.26	5.76	9.24	3.18
Or	0.56	2.72	0.56	1.67	1.11	6.67	8.34	2.22
Ab	8.91	8.38	23.06	16.24	20.44	23.44	24.63	18.34
An	57.27	36.97	36.97	44.20	45.59	35.03	27.52	41.98
Cor	—	—	—	—	—	—	—	—
Di	12.06	18.30	12.17	17.39	3.76	6.67	9.02	7.20
Hy	11.56	19.40	13.12	9.18	26.53	18.28	15.38	21.42
Ol	1.90	—	—	6.01	—	—	—	—
Il	1.82	9.73	3.04	1.52	0.61	1.37	2.43	1.52
Mt	5.57	2.78	8.82	2.09	0.46	2.09	2.78	2.55
Ap	—	—	—	0.34	—	—	0.33	0.33
Py	—	—	0.24	0.12	—	—	—	—

comparing the variation diagrams with those of other calc-alkali complexes (Reference 8). It will be seen that these characteristics, particularly of the gabbros, place drastic limits on the possible modes of origin for these rocks.

Larsen (Reference 8) showed that, except for minor systematic differences such as those mentioned above, the rocks of the southern California batholith yield smooth variation curves which resemble closely those of other calc-alkali complexes. Also Nockolds and Allen (Reference 12) demonstrated that the triangular plot $K_2O + Na_2O - Fe_2O_3 + FeO - MgO$ for the batholith adheres to the trend characteristic of the series elsewhere. Similarly, these systematic relations are also shown by the triangular plot $K_2O + Na_2O - FeO - MgO$, as shown in Figure 1. This plot has the advantage of exhibiting unambiguously the important parameter $Fe^{2+}/(Mg + Fe^{2+})$, which, as will be seen later, varies directly in response to changes in the oxygen fugacity.

To the extent that the data points of Figure 1 represent successive liquids, a path of crystallization is defined by the curve. As has been frequently mentioned in the literature, this curve differs strikingly from a similar plot for the gabbroic complexes. However, there is considerable evidence that a complete spectrum of curves exists between the two extremes (Reference 13). It is also apparent that the curvature exhibited is of the type expected when increasingly iron-rich ferromagnesian silicates, whose compositions lie on the $FeO - MgO$ join, separate from the melt. If this is the case, the scatter of points on either side of the curve is seen as deviation from

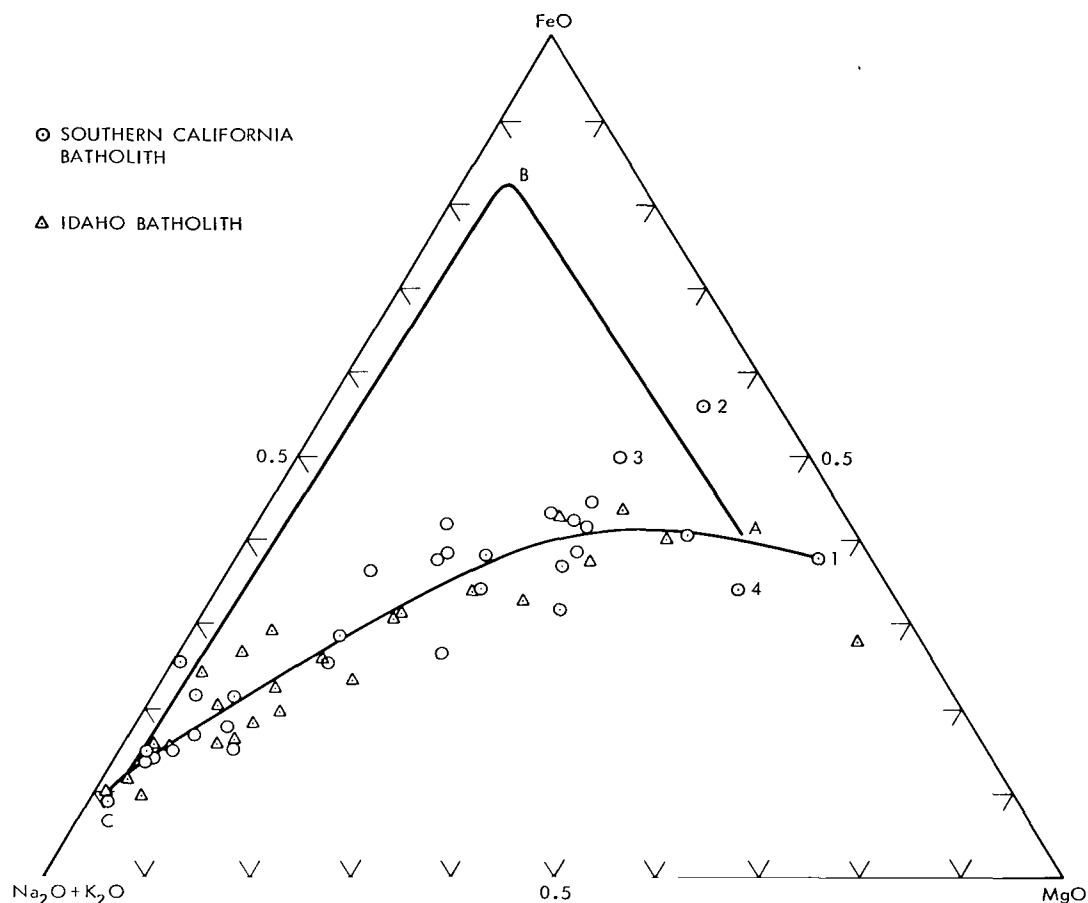


Figure 1—Variation in weight fractions for rocks of the Southern California and Idaho batholiths (curve AC) and the Skaergaard complex (curve ABC). Numbers refer to specimens in Tables 1, 2, and 3. Data from Wager and Deer (Reference 1), Larsen (Reference 8), Larsen and Schmidt (Reference 19), and Hietanen (Reference 17).

possible liquid compositions caused by (1) interactions with early-formed rocks, perhaps represented by cognate inclusions, or (2) varying proportions of liquid differentiate and accumulated crystalline precipitates. We shall see, however, that there is little or no chemical evidence of reaction with the country rocks.

As has frequently been stressed, such diagrams usually exhibit the greatest scatter near the FeO–MgO join, since the rocks which fall in this region tend to represent crystal cumulates rather than liquids. Thus the variation curve would ordinarily not be extended to the right of point A in Figure 1. If, however, as was inferred by Miller (Reference 11), the troctolite (No. 1) represents the liquid line of descent, the curve should be extended toward point 1 as shown. That some of the scatter of Figure 1 is attributable to crystal cumulates is at least suggested by such specimens as Nos. 2 and 3, which exhibit abnormally high values of $\text{Fe}^{2+}/(\text{Mg} + \text{Fe}^{2+})$ because they contain large amounts of iron-titanium ores (Table 2).

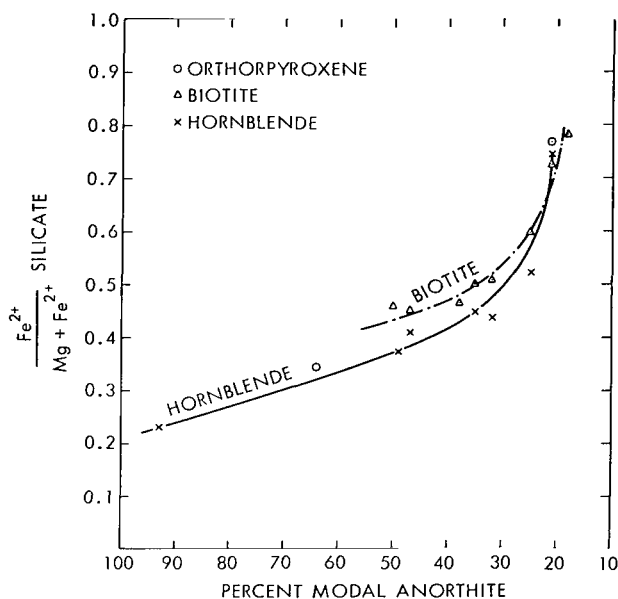


Figure 2—Variation of mineral compositions from the Southern California batholith. Data from Larsen and Draisin (Reference 14).

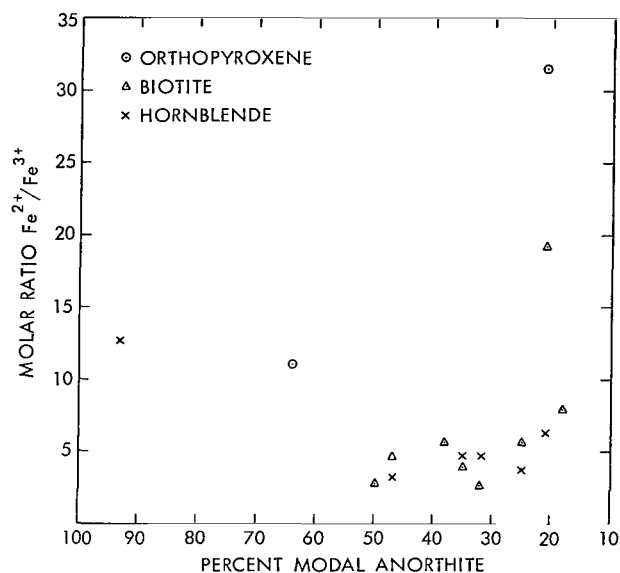


Figure 3—Variation of ferrous/ferric ratios from minerals of the Southern California batholith. Data from Larsen and Draisin (Reference 14).

The systematic variation of $\text{Fe}^{2+}/(\text{Mg} + \text{Fe}^{2+})$ evident from Figure 1 is more informatively displayed in Figure 2, which is a plot of the mineral phases involved (Reference 14). This figure exhibits a similar increase in $\text{Fe}^{2+}/(\text{Mg} + \text{Fe}^{2+})$ as a function of the anorthite content for all ferromagnesian silicates. While it is unlikely that the coexisting minerals (as indicated by points with the same horizontal coordinates) represent perfect equilibrium (Reference 15), it is clear that equilibrium was approached to the degree that the mineral compositions kept essential pace with each other as differentiation progressed. The steep slope and strong positive curvature of the curves may be interpreted to mean that the ferromagnesian minerals were precipitating at an increasing ratio to the precipitating plagioclase. We shall see that such behavior is to be expected if the liquidus temperatures of the feldspar and ferromagnesian components diverge.

Since there should also be a relation between the degree of differentiation and the ratio $\text{Fe}^{2+}/\text{Fe}^{3+}$, the latter has been plotted as a function of the anorthite content in Figure 3. It is obvious that in this case the relationship is somewhat more complex. We shall see that such behavior is not unexpected when account is taken of the complex coupled reactions involving ferric iron both within the melt and in the crystalline phases.

Sierra Nevada and Idaho Batholiths

These large complexes of multiple intrusions bear many resemblances to the Southern California batholith. As with it, the time sequence of emplacement leads from gabbro to granite, although the mean compositions in these cases are nearer granodiorite and quartz monzonite.

For the Idaho batholith there are similar areas of metamorphic gneisses exhibiting evidence of widespread metasomatism (Reference 16) and of both synkinematic and postkinematic plutons (Reference 17). However, there is evidence that much of the Sierra Nevada batholith is post-kinematic in structure (Reference 18).

As pointed out by Larsen (Reference 8) and by Larsen and Schmidt (Reference 19), the oxide abundances of both the Sierra Nevada and Idaho batholiths adhere to smooth variation curves very similar to those of the Southern California batholith. There is also considerable quantitative correspondence between the Idaho and Southern California rocks, as may also be seen from Figure 1. However, the Sierra Nevada rocks appear to be slightly higher in K_2O and differ enough systematically so that they must be represented by a different variation curve, as is done in Figure 4. A limited number of chemical analyses of the ferromagnesian minerals from the Idaho batholith (Reference 19) indicate a trend similar to that shown in Figure 2. Although no similar data are available for the Sierran rocks, it is clear that the ferromagnesian minerals of the specimens represented in Figure 4 would also show this trend, since none of the rocks contain enough Fe_2O_3 to make oxide phases a perturbing factor.

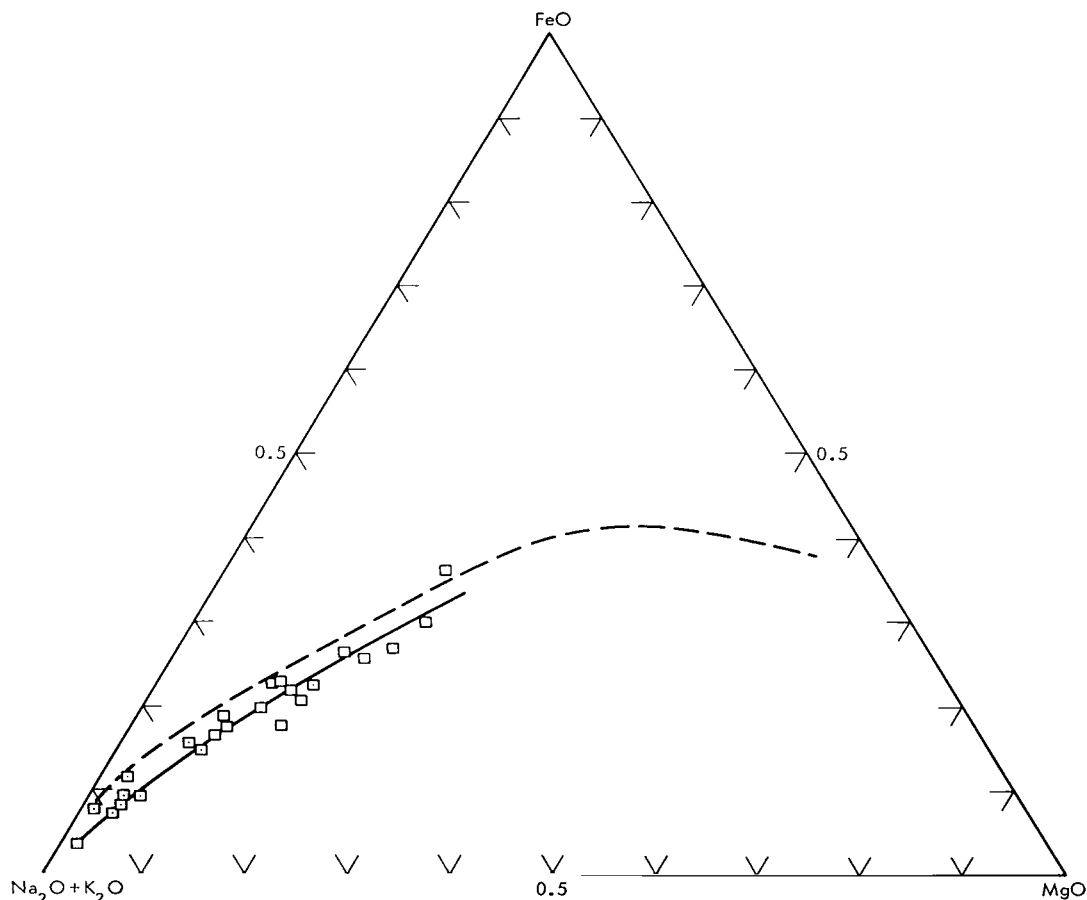


Figure 4—Variation in weight fractions for rocks of the Sierra Nevada batholith. Data from Bateman, et al. (Reference 18). Dashed line is for Southern California and Idaho batholiths.

Other Plutonic Complexes

Although the writer knows of no additional mineral chemical studies of the scope of those of Larsen and Draisin (Reference 14), a variety of data indicates that quite generally the parameter $\text{Fe}^{2+}/(\text{Mg} + \text{Fe}^{2+})$ increases strikingly as differentiation proceeds. This is shown by a limited number of mineral analyses from the small calc-alkali plutons such as the Garabal Hill-Glen Fyne complex of Scotland (Reference 20) and the Guadalupe igneous complex of California (Reference 21). It is also shown by the more alkaline White Mountain magma series (Reference 22). A similar variation diagram, virtually identical to Figures 1 and 4, is shown by the smaller Bald Rock batholith of northeastern Oregon (Reference 23). Then too, if a variety of chemical analyses of ferromagnesian minerals, such as appear in Johannsen (Reference 24), for example, are examined, it will be seen that on the whole the most ferrous-iron-rich representatives of each species will be found in rocks which resemble late igneous differentiates. This is brought out in particular by such granites as that at Cape Ann, Massachusetts, which has some of the most iron-rich biotite recorded in the literature.

It is interesting also that the oxides which accompany the iron-enriched silicates are always magnetic or iron titanium oxides in which hematite occurs only as a minor solution component. For the Guadalupe complex (Reference 21), the ilmenites show a marked increase in both $\text{Fe}^{2+}/(\text{Mg} + \text{Fe}^{2+})$ and in $\text{Fe}^{2+}/\text{Fe}^{3+}$ of the granites as compared with the same quantities in the gabbros.

Volcanic Complexes

The rocks of the calc-alkali volcanic complexes usually exhibit variation curves very similar to those of their plutonic equivalents. This is especially true for the rock-forming oxides of elements other than iron. It is also true for the triangular alkali- $\text{Fe}_2\text{O}_3 + \text{FeO}$ - MgO plots (Reference 12) and in many cases for plots such as Figures 1 and 4 as well. However, in detail there may be great deviations from systematic change in $\text{Fe}^{2+}/(\text{Mg} + \text{Fe}^{2+})$ of the minerals. Thus Larsen and Cross (Reference 25) noted that in the San Juan volcanics of Colorado the ferromagnesian minerals of late differentiates are frequently enriched in MgO and Fe_2O_3 and that the phenocrysts of hornblende and biotite are on extrusion altered to oxyhornblendes and oxybiotites. From such observations it can be inferred that, while the major differentiation trends of volcanic rocks might be established under plutonic conditions, wide deviations may occur in individual specimens during this late extrusive history. This effect would be expected to be particularly strong in acid, water-rich magmas which are undergoing vesiculation and disruption, since it may be shown (Reference 26) that under these circumstances the reactions involving hydrous ferromagnesian silicates are oxidizing and lead to a decrease in $\text{Fe}^{2+}/(\text{Mg} + \text{Fe}^{2+})$ in both the crystals and melt.

When, however, lavas are rapidly extruded and cooled with a minimum of volatile escape and disruption, they may form phenocryst-bearing glasses in which the plutonic state of reduction has been retained. This is the case, for example, for hornblende and biotite phenocrysts of glassy

flows in the San Juan rocks. It is also true for olivine and pyroxene phenocrysts in many acid glasses of the British Isles and Iceland (Reference 27). In fact, in some of the latter rocks, $\text{Fe}^{2+}/(\text{Mg} + \text{Fe}^{2+})$ of olivine exceeds 0.8, which, as will be seen later, corresponds to highly reducing conditions.

Summary of Observations

It seems quite conclusive that in both the plutonic and volcanic calc-alkali complexes there is a strong tendency for $\text{Fe}^{2+}/(\text{Mg} + \text{Fe}^{2+})$ of both the minerals and melt to increase systematically through the sequence gabbro-granite (and basalt-rhyolite) and that deviations from this trend in certain volcanic rocks are easily understood. Furthermore, the characteristic oxide phases with which the ferromagnesian minerals are associated throughout the sequence are ferrite- and ferrous-iron-titanium oxides. Hematite is rare or lacking in the plutonic rocks, but may occur as a near-surface oxidation product in volcanics.

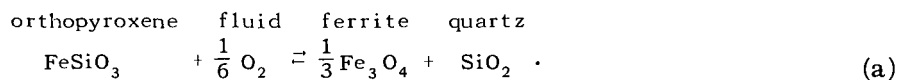
In addition to these systematic mineral compositional variations, the calc-alkali series may have local systematic bulk compositional characteristics, such as low K_2O , which may serve as useful indicators of the origin of the series.

OXIDATION STATES OF MAGMATIC MINERALS AND MAGMAS

Mineral Indicators of P_{O_2}

Examination of a variety of igneous and metamorphic rocks has shown that the atomic fraction $\text{Fe}^{2+}/(\text{Mg} + \text{Fe}^{2+})$ of the ferromagnesian minerals is a reliable indicator of the oxygen fugacity P_{O_2} of the environment if proper account is taken of other components (Reference 26).

In the gabbroic rocks, which are undersaturated with respect to silica, the oxygen fugacity may be related directly to the composition of coexisting olivines, pyroxenes, and ferrites (Reference 28) or alternatively to the coexisting iron-titanium oxides (Reference 29). In the silica-saturated rocks such as characterize the calc-alkali series, it is possible also to utilize certain reactions involving free silica. An example which is useful in the present case is the following:



It will be observed (Table 2) that all the phases which enter into this reaction are present in certain of the gabbroic rocks and the granite. Consequently, if (as we have every reason to believe), these phases crystallized at solidus or near-solidus temperatures, they should give a reliable indication of the oxidation state prevailing at the time crystallization occurred.

The equation of equilibrium for reaction (a) may be written as

$$\log P_{O_2} = -6 \log K_a - 6 \log X_{Fe}^{px} + 2 \log \alpha_{Fe}^{fr} + \frac{6P\Delta V_a}{2 \cdot 303RT} \quad (1)$$

The quantities which appear in this equation are defined as follows:

P_{O_2} = oxygen fugacity

K_a = equilibrium constant, a function of the temperature only

X_{Fe}^{px} = atomic fraction $Fe^{2+}/(Mg + Fe^{2+})$ in orthopyroxene

α_{Fe}^{fr} = relative activity of Fe_3O_4 in ferrite

P = the total pressure

ΔV_a = the difference in volume between the solid reactants and products

R = gas constant

T = absolute temperature in ° Kelvin.

In Equation 1 it has been assumed that orthopyroxene behaves as an ideal solution in this temperature range (Reference 30). Unfortunately, there is no explicit way of evaluating α_{Fe}^{fr} . It is known (References 29 and 31) that in ferrite Fe_3O_4 is combined largely with Fe_2TiO_4 (ulvospinel). The data of Buddington and Lindsley (Reference 29) show that in the low temperatures (900° to 1000°K) of magmatism, corresponding to water-rich granites and pegmatites, the mole fraction of Fe_3O_4 in ferrite falls in the range of 0.8 to 0.9 and that at subsolidus temperatures it is somewhat higher. We shall see that for all practical purposes these values correspond to $\alpha_{Fe}^{fr} \rightarrow 1$. On the other hand, for the high-temperature (~1300°K) ferrogabbros of the Skaergaard intrusion, these authors inferred that this mole fraction lies between 0.3 and 0.2. It will be necessary to take into account these effects on the activity of Fe_3O_4 in evaluating Equation 1.

The orthopyroxenes and ferrites which enter into reaction (a) also contain constituents other than the major components. Although the quantities of these constituents present in the ferrites of the southern California rocks are not known, the orthopyroxenes from these rocks contain quantities of CaO , Al_2O_3 , Fe_2O_3 , TiO_2 , MnO , and Na_2O which aggregate about 10 percent by weight. For ferrites from other areas, the quantity of minor components is generally in the range of 5 percent. The effect of these constituents on the equilibria is difficult to evaluate, but element distribution studies (Reference 30) indicate that for the pyroxenes this effect is largely one of simple dilution. Buddington and Lindsley (Reference 29) disregarded these minor constituents by recalculating the major components to 100 percent, and this is also done here. If indeed the effect of the minor constituents is largely one of dilution, then Equation 1 shows that both X_{Fe}^{px} and α_{Fe}^{fr} will be reduced so that a certain amount of cancellation occurs.

Now ΔV_a is approximately 4.8 cm^3 under STP conditions so that the fourth term on the right side of Equation 1 is approximately $0.152 P/T$. Thus in the range of magmatic temperatures and

for pressures up to 10^4 atm, $\log P_{O_2}$ will shift a maximum of approximately 1.5 units because of pressure variations. Since, as we shall see, this is also less than the uncertainty from K_a , we may omit the fourth term and write Equation 1

$$\log P_{O_2} = -6 \log K_a - 6 \log X_{Fe}^{Px} + 2 \log a_{Fe}^{fr} \quad (2)$$

We shall consider first the pure iron silicate reference state when $X_{Fe}^{Px} = a_{Fe}^{fr} = 1$. To calculate K_a as a function of T , we may use the standard heats of formation for Fe_3O_4 and SiO_2 as compiled by Robie (Reference 32) and the corresponding enthalpy and entropy changes for these same constituents and O_2 as given by Kelley (Reference 33). Analogous data are also available for $FeSiO_3$ from the experimental work of Lindsley, MacGregor, and Davis (Reference 34) and Lindsley, Spidel, and Nafziger (Reference 35) and from the calculations of Olsen and Fuchs (Reference 36). The results are given in terms of $\log K_a$ in Table 4 and are plotted in Figure 5 in terms of $\log P_{O_2}$. The stability fields of phases in the system Fe-O are also shown (by the outer, unlabeled lines) for comparison.

Unfortunately, because of the unknown uncertainties introduced by $FeSiO_3$, it is not possible to estimate the total uncertainty in the data of Table 4. We may, however, reason by analogy with the reaction

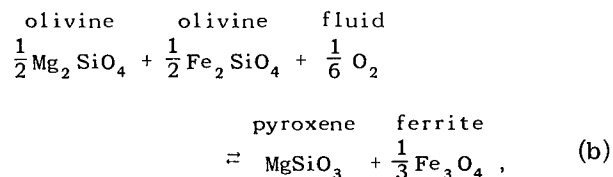


Table 4

Logarithm of the Equilibrium Constant of Reaction (a) As a Function of the Temperature.

T°K	Log K_a
400	9.96
500	7.40
600	6.04
700	4.80
800	4.11
900	3.47
1000	2.81
1100	2.47
1200	2.14
1300	2.00
1400	1.67

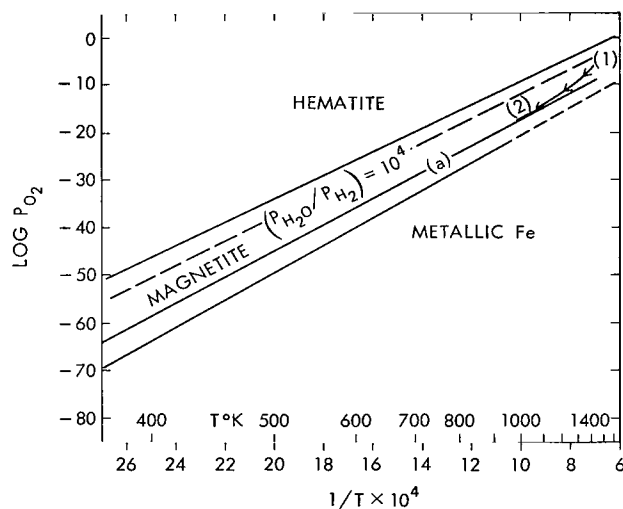


Figure 5—Variation of the oxygen fugacity as a function of the temperature for some systems involving iron. Curve (a) represents the oxidation of pure $FeSiO_3$ to Fe_3O_4 , while the other solid lines represent phase boundaries in the system Fe-O. The dashed line refers to the system H-O for the composition defined by $(P_{H_2O}/P_{H_2}) = 10^4$. The curve (1)-(2), on the other hand, is deemed a possible path of crystallization for calc-alkali series magmas.

which should exhibit essentially the same energetics as (a), since both reactions are dominated by the very energetic oxidation of FeO to Fe_3O_4 . If this analogy is followed, it is found that $\log K_b$ for 1400°K is 1.83 and for 400°K the corresponding value is 10.25. Comparison with Table 4 shows that these values are close, even surprisingly close, to $\log K_a$ for the same temperatures, and this also holds for intermediate temperatures (Reference 28). Even the slightly greater values of $\log K_b$ are explicable in terms of the increased affinities imparted to reaction (b) by the conversion of Mg_2SiO_4 to MgSiO_3 . While this correlation does not prove that curve (a) is accurate, it at least indicates that it is consistent with other, more accurate data.

The important feature of curve (a) in Figure 5 is not in fact its precise location, which might be off by several units in $\log P_{\text{O}_2}$, but rather its slope, or the run of the curve with temperature, since this trend line establishes the relative changes we wish to measure.

It is clear from Equation 2 that as MgO is added or FeO subtracted (as in oxidation of FeO to Fe_3O_4) $X_{\text{Fe}^{\text{px}}}$ diminishes and $\log P_{\text{O}_2}$ for reaction (a) is displaced toward the magnetite-hematite boundary, as is quite generally true for reactions which involve ferrous-iron silicates and higher oxide phases (Reference 28). This effect may be countered in part by the simultaneous presence of Fe_2TiO_4 in the ferrite so that $a_{\text{Fe}^{\text{fr}}}$ is thereby reduced from its value of unity in pure magnetite. Although little is known of the behavior of $a_{\text{Fe}^{\text{fr}}}$ as a function of the composition, it is believed (Reference 29) that unmixing occurs within the system. If this is true, then $X_{\text{Fe}^{\text{fr}}} < a_{\text{Fe}^{\text{fr}}} < 1$ for all stable configurations of the phase diagram, where $X_{\text{Fe}^{\text{fr}}}$ is the mole fraction of Fe_3O_4 in ferrite. Consequently, $X_{\text{Fe}^{\text{fr}}}$ should provide an upper limit for the effect of Fe_2TiO_4 on reaction (a).

We may illustrate the simultaneous effects of variations of FeSiO_3 and Fe_3O_4 by considering the early gabbroic differentiates typical of both the calc-alkali and gabbroic complexes. For these differentiates, $X_{\text{Fe}^{\text{px}}} \sim 0.2$, a value which shifts $\log P_{\text{O}_2}$ of reaction (a) 4.19 units toward the magnetite-hematite boundary (Figure 5). Now the diminishing of Fe_3O_4 by the presence of Fe_2TiO_4 in ferrite will have the opposite effect. In fact, if we imagine $X_{\text{Fe}^{\text{fr}}}$ to assume the extreme (nonequilibrium) value of 0.2, $\log P_{\text{O}_2}$ for reaction (a) is moved a maximum of 1.4 units to lower values. The contrast in the magnitude of the two effects is, of course, a consequence of the different coefficients of $\log a_{\text{Fe}^{\text{fr}}}$ and $\log X_{\text{Fe}^{\text{px}}}$; $\log P_{\text{O}_2}$ is more sensitive to changes in the latter. However, such arbitrary changes do not satisfy equilibrium requirements, which demand the simultaneous mutual adjustment of ilmenite, magnetite, and silicate compositions. In fact, the data of Buddington and Lindsley (Reference 29) indicate that equilibrium values of $X_{\text{Fe}^{\text{fr}}}$ between 0.2 and 0.3 occur with quite iron-rich silicates at gabbroic liquidus temperatures. Thus there is very good correspondence between their results from the iron-titanium oxides and deductions from Equation 2.

Similarly, if we consider the effect of $X_{\text{Fe}^{\text{fr}}} = 0.8$ in the range of granitic liquidus temperatures, we see that this value shifts $\log P_{\text{O}_2}$ of reaction (a) only 0.19 units closer to curve (a) than is implied by $a_{\text{Fe}^{\text{fr}}} = 1$. Consequently, we should expect that the rocks of the southern California batholith would plot above curve (a) and that with falling temperature they would approach this curve asymptotically, as is indicated by the path (1)-(2) in Figure 5.

In any event it seems likely that, in the differentiation series gabbro-granite, $\log P_{O_2}$ must decrease at least as rapidly as along curve (a). Furthermore, because of distribution relations between coexisting minerals, this change in P_{O_2} will be equally well reflected in the increase of $Fe^{2+}/(Mg + Fe^{2+})$ of other minerals, as is in fact implied by Figure 2.

Both the mineral compositional data and the rock variation diagrams thus indicate that, contrary to previous suggestions, the fugacity of oxygen decreases during crystallization differentiation. Actually this effect might already have been anticipated, as was pointed out by Best and Mercy (Reference 21), by considering the oxide phases which are present in granite. If P_{O_2} should remain constant or increase during differentiation, it is clear from Figure 5 that the field of hematite would be entered at approximately $T = 1200^\circ K$, which corresponds to diorite or tonalite. Thus all granites should be hematite-bearing, a relationship which is certainly far from true.

This result is also in agreement with those obtained from the iron-titanium oxides by Buddington and Lindsley (Reference 29). Although many of their specimens suggest superimposed regional metamorphism, values of $\log P_{O_2}$ obtained from granites and pegmatites generally fall in the range of -18 for $T \sim 900^\circ K$ and -14 for $T \sim 1000$. Furthermore, at least some of these granites contain very ferrous-iron-rich silicates, so that they correspond rather closely to curve (a) of Figure 5.

Although Best and Mercy (Reference 21) pointed out the above anomalies with respect to the oxide phases, their interpretation of the Guadalupe complex differs in important ways from the one which is adopted here. One reason for this difference is that they attempted to assign one oxidation state to the whole complex without considering the effect of temperature change and differentiation as reflected in the fraction $Fe^{2+}/(Mg + Fe^{2+})$. The necessity for taking this effect into account will be equally apparent when the melt is considered.

Oxidation States of Silicate Melts

There are various ways in which the oxidation states of melts may be discussed; the one chosen is merely a matter of convenience. However, we are concerned here not only with the interactions of the anhydrous oxide components but also with the dissolved volatiles and most particularly with those in the subsystem H-O; although other species involving sulfur, carbon, etc., will be present.

We shall consider first the behavior of the subsystem H-O in isolation from the melt to see how its state of oxidation depends on the temperature and the pressure.

The pertinent reaction then is



If the composition lies between H_2O and O_2 , corresponding to a high state of oxidation not ordinarily attained in petrologic systems, then it is apparent that the oxygen fugacity P_{O_2} will be

approximately proportional to the gas pressure. If, however, the composition of the system lies between H_2 and H_2O , as is actually the case in most plutonic environments, then we proceed as follows: Let β equal the number of original moles of H_2 in excess of the hydrogen in $2H_2O$ and α the number of moles of O_2 formed by reaction (c). Then, if a perfect gaseous mixture is assumed, the equation of equilibrium may be written as

$$K_c = \frac{P_{H_2}^2}{P_{H_2O}^2} P_{O_2} = \left(\frac{2\alpha + \beta}{2 - 2\alpha} \right)^2 P_{O_2} \quad (3)$$

If α is assumed to be negligible compared to β (as is usually the case), then

$$\frac{4K_c}{\beta^2} = P_{O_2} \quad (4)$$

so that P_{O_2} is inversely related to the square of the excess hydrogen but is independent of the total pressure.

On the other hand, if β is negligible compared to α , so that virtually all O_2 and H_2 come from the decomposition of water, it may be shown that

$$K_c \left(\frac{2 + \alpha}{\alpha} \right) \left(\frac{1 - \alpha}{\alpha} \right)^2 = P \quad (5)$$

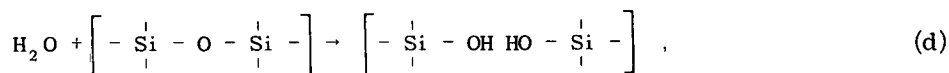
where P is the total gas pressure. It is clear that in this case the extent of decomposition α , and hence P_{O_2} , is a function of P as well as of the temperature.

If we turn to the most significant case, that represented by Equation 4, we may use thermochemical data (Reference 37) to calculate $\log P_{O_2}$ as a function of T for any given values of P_{H_2O}/P_{H_2} . This function, which is nearly linear on the $1/T$ scale, is shown for $(P_{H_2O}/P_{H_2}) = 10^4$ in Figure 5. In general, such curves of constant P_{H_2O}/P_{H_2} ratios are subparallel to the phase boundaries and reaction curves such as (a). Consequently, it might be expected that, in systems dominated by gases in the composition range H_2-H_2O , $\log P_{O_2}$ would drop markedly with the temperature, so that fluids of this type are far from oxidizing in character when compared to those invoked by Osborn (Reference 4).

This picture will, of course, be modified by the fact that the gases may deviate considerably from perfect mixtures, especially through interaction with such species as SO_2 , H_2S , CO_2 , CO , etc., in the natural system. Indeed Nordlie (Reference 38) has shown, through corrections of natural gas analyses from Hawaiian volcanoes, that SO_2 and CO_2 are as important as H_2O just before basalt is extruded. We shall find, however, that there is evidence that the role of water is greatly enhanced as differentiation proceeds.

We must now consider what happens when the subsystem H-O interacts with the melt, a process which will further modify the conclusions arrived at above. For this it is instructive to consult the work of Wasserburg (Reference 39) and of Shaw (Reference 40) on the energetics of such melts.

In his study, Wasserburg found that the depression of the melting point in the system $\text{NaAlSi}_3\text{O}_8\text{-H}_2\text{O}$, as given by the data of Goranson (Reference 41), could be accounted for if it were assumed that H_2O reacted strongly with the silicate component according to the following scheme:



in which the bridging oxygen in the Si-O framework is replaced by OH. Under these circumstances, the chemical potentials of H_2O and $\text{NaAlSi}_3\text{O}_8$ are given by the following expressions:

$$\mu_{\text{H}_2\text{O}} = \mu_{\text{H}_2\text{O}}^\circ (T, P) + RT \ln \left\{ \frac{X_{\text{H}_2\text{O}} f_{\text{H}_2\text{O}}}{X_{\text{H}_2\text{O}} + r X_{\text{Ab}}} \right\} \quad (6)$$

and

$$\mu_{\text{Ab}} = \mu_{\text{Ab}}^\circ (T, P) + r RT \ln \left\{ \frac{r X_{\text{Ab}} f_{\text{Ab}}}{X_{\text{H}_2\text{O}} + r X_{\text{Ab}}} \right\} \quad (7)$$

In these expressions, the quantities μ° , X , and f , represent the standard chemical potentials, mole fractions, and activity coefficients, respectively, in the melt; and r is the number of bridging oxygens per formula unit. In his original development, Wasserburg (Reference 39) found that the data could be approximated with $f_{\text{H}_2\text{O}} = f_{\text{Ab}} = 1$, so the solution as defined by the model was essentially ideal. Under this interpretation, H_2O interacts with the Si-O framework of the melt about as energetically as the oxygen does, so there is no excess free energy when H_2O breaks the Si-O bridges according to reaction (d). However, examination by Shaw (Reference 40) of these and additional data in the system $\text{CaAl}_2\text{Si}_2\text{O}_8\text{-KAlSi}_3\text{O}_8\text{-NaAlSi}_3\text{O}_8\text{-SiO}_2\text{-H}_2\text{O}$ found that generally a negative excess energy term is required to fit the data so that the f 's are less than unity. Thus there is evidence that generally the interaction of water with the silicate melt is even more energetic than is implied by the ideal dissociation model of Wasserburg.

There is no corresponding evidence for the behavior of H_2 in silicate melts, but we shall see that there is considerable experimental evidence that generally the ferromagnesian silicates react less energetically with water than do the quartzo-feldspathic constituents as discussed above. However, there is an important reaction involving both H_2 and H_2O which directly influences the

state of oxidation:



The equation of equilibrium for this reaction is

$$\frac{a_{\text{H}_2\text{O}}}{a_{\text{H}_2}} K_e = \left(\frac{a_{\text{FeO}_{3/2}}}{a_{\text{FeO}}} \right)^2 \quad (8)$$

where the a 's refer to the relative activities in the melt of the components indicated by the subscripts. We have seen that H_2O reacts strongly with the melt and that this tendency is likely to increase as differentiation proceeds. We know of no corresponding reaction for H_2 ; and, although reaction (e) tells us that this volatile can react with ferric iron, it is clear that during differentiation this possibility decreases with the steady decrease in the absolute quantity of ferric iron. As a consequence, it seems highly likely that the ratio $a_{\text{H}_2\text{O}}/a_{\text{H}_2}$ decreases during differentiation and that $\log P_{\text{O}_2}$ must decrease faster with temperature than the line defined for constant $P_{\text{H}_2\text{O}}/P_{\text{H}_2}$. Thus it is likely that a curve something like (1)-(2) of Figure 5 would be adhered to.

Although $\log P_{\text{O}_2}$ may well have decreased as stated above, the behavior of the $\text{Fe}^{2+}/\text{Fe}^{3+}$ ratio is more difficult to deduce. In the first place, the behavior of K_e is not known with any confidence; and, second, it might be expected that both $\text{FeO}_{3/2}$ and FeO would form somewhat non-ideal solutions in the melt. It is easy to show that equally serious complications arise when the $\text{Fe}^{2+}/\text{Fe}^{3+}$ ratios of the mineral phases are considered, for in this case the reactions involve complicated coupling between the species FeO , $\text{FeO}_{3/2}$, $\text{AlO}_{3/2}$, and SiO_2 . This is why the relatively large scatter of $\text{Fe}^{2+}/\text{Fe}^{3+}$ in Figure 3 is not unexpected and why the parameter $\text{Fe}^{2+}/(\text{Mg} + \text{Fe}^{2+})$ is more suitable than $\text{Fe}^{2+}/\text{Fe}^{3+}$ as an index to the oxidation state of the system.

There are only a few experimental data which bear on this problem. Some of the most pertinent of these are the experiments of Fudali (Reference 42) to determine the equilibrium oxygen fugacity of various basalts and andesites. In these experiments, which were carried out at 1473°K at one atmosphere total pressure, gas mixing apparatus was used to achieve a variety of oxygen fugacities over molten specimens of basalt and andesite. The resulting $\text{Fe}^{2+}/\text{Fe}^{3+}$ equilibrium ratios were then compared with the original ratios of the rocks to obtain the P_{O_2} under which the rocks formed. Although there are many complications in such a procedure, it has been pointed out (Reference 26) that the oxidation state of an extrusive magma is frequently quite different from the original state under plutonic conditions. In fact, when Fudali's observed values of $\log P_{\text{O}_2}$ are plotted against SiO_2 , there is only a scatter of points about a horizontal line. It is possible that this failure to observe a clear-cut trend is attributable to a lower temperature of crystallization of the original andesites as compared with the basalts. However, it is also possible that the andesites were more subject to interaction with the atmosphere because of greater viscosities and volatile contents.

CONSEQUENCES OF THE DIFFERENTIAL SOLUBILITIES OF THE SILICATES

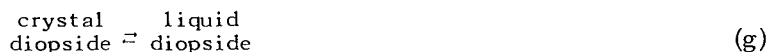
We have already discussed the interaction of water and the silicate melt and have used it to account for the progressive reduction of the magma as differentiation proceeds. We must now consider what effect this interaction has upon the course of differentiation itself. This question may best be discussed in terms of the influence of water on the solubility of the silicates in the melt.

The effect of water on the solubilities of certain silicate systems is well known, as documented in the papers already referenced. In particular, the system $\text{CaAl}_2\text{Si}_2\text{O}_8\text{--KAlSi}_3\text{O}_8\text{--NaAlSi}_3\text{O}_8\text{--SiO}_2\text{--H}_2\text{O}$ shows profound depression of the liquidus temperatures as the quantity of dissolved water is increased (References 43 and 44). However, in the present case, we need to compare the solubility of this quartzo-feldspathic subsystem with that of the ferromagnesian subsystem. Fortunately, a direct comparison is afforded by the experiments of Yoder and Tilley (Reference 45) on natural basalt systems. These experiments show clearly that, whereas water pressure increases the solubility of plagioclase profoundly, the effect on the ferromagnesian components is much more modest. For example, in the case of an olivine tholeite basalt, 2,000 bars H_2O pressure depresses by as much as 250°K the temperatures at which plagioclase begins to crystallize, while the corresponding temperatures for the crystallization of olivine and pyroxene are depressed less than 100°K . Furthermore, although the greatest depression of these temperatures occurs in the first 2,000 bars, the disparity between the plagioclase and ferromagnesian liquidus temperatures continues to increase up to at least 10 kilobars.

A direct comparison in the simpler system $\text{CaAl}_2\text{Si}_2\text{O}_8\text{--CaMgSi}_2\text{O}_6\text{--H}_2\text{O}$ is also given by the experiments of Yoder as quoted by Clark (Reference 46). A diagram therein shows that 5,000 bars water pressure depresses the melting point of diopside somewhat less than 100°K , while the corresponding depression for anorthite is in excess of 300°K . This has the effect of shifting the eutectic markedly toward anorthite, so that the stability field of this mineral is considerably decreased. For our purposes it is informative to examine this behavior in terms of the previously discussed energetic model. The reactions are:



and



which have the equilibrium equations

$$K_{\text{An}} = X_{\text{An}}^{\text{L}} f_{\text{An}}^{\text{L}} \quad (9)$$

and

$$K_{Di} = X_{Di}^L f_{Di}^L . \quad (10)$$

Here X_{An}^L and X_{Di}^L are the mole fractions of anorthite and diopside in the melt, and the f 's are the corresponding activity coefficients.

Equations 9 and 10 may be written in an alternative way that further elucidates the situation:

$$K_{An} = (X_{An}^L)^n , \quad (11)$$

$$K_{Di} = (X_{Di}^L)^m , \quad (12)$$

where n and m are small numbers but not necessarily integers. It may easily be shown that if the solutions are of the ideal dissociated type discussed by Wasserburg (Reference 39), the chemical potentials of the components are of the form of Equation 7. In the present case, which refers to the feldspar structure, n is an integer, while the X^L terms refer to the mole fractions of dissociated silicate components (Reference 40).

We may apply Equations 9 and 10 or 11 and 12 to an isothermal section above the cotectic temperature of the T - P_{H_2O} - X surface. Then K_{An} and K_{Di} refer to the same temperature and we may write

$$\frac{f_{Di}^L}{f_{An}^L} \left(\frac{K_{An}}{K_{Di}} \right) = \frac{X_{An}^L}{X_{Di}^L} . \quad (13)$$

Although we do not know precisely the effect of pressure on K_{An}/K_{Di} , we may infer that it will be small relative to the effect of water already discussed, since it depends upon the volume change produced by melting of the pure constituents. The effect of hydrostatic pressure on the melting relations of the system anorthite-albite-diopside has been discussed recently by Lindsley and Emslie (Reference 47), who found that the phase boundary was shifted toward anorthite. However, no simple correlation can be made between this behavior of the anhydrous system and the effect of water, since, as we have seen, the latter constituent completely changes the structure of the melt. In any case, the effect of pressure on the anhydrous system is less than 1/3 that of water discussed above.

It is clear from the experimental data of Yoder (Clark, Reference 46) that as P_{H_2O} is increased X_{An}^L/X_{Di}^L must increase, since the anorthite liquidus is displaced more toward anorthite than the diopside liquidus is toward diopside. Consequently, if K_{An}/K_{Di} decreases only slightly because of hydrostatic pressure, f_{Di}^L/f_{An}^L must increase to adjust to the relatively large increase

in x_{An}^L/x_{Di}^L . In terms of Equations 11 and 12, this relationship corresponds to a faster growth of n than of m with P_{H_2O} . In energetic terms, it is equivalent to a greater increase in negative excess free energy of solution for anorthite than for diopside. We thus see a direct connection between the differential solubilities of the feldspathic and ferromagnesian components and the energies of their respective interactions with water. Indeed there is further experimental evidence from the system $CaAl_2Si_2O_8-NaAlSi_3O_8-KAlSi_3O_8-H_2O$ (Reference 44) that an even finer distinction can be drawn between the solubilities of anorthite and albite to show that the latter component will tend to be relatively more concentrated in the water-rich melt.

It is clear from the foregoing that although the differentiation trends in the gabbroic and calc-alkali series are not easily distinguishable in terms of oxidation states, the effects of different water contents on the mineral solubilities should be very great indeed. Particularly, the greater tendency for water to react exothermically with the quartzo-feldspathic constituents than with the ferromagnesian constituents and the tendency for this effect to increase with acidity bring about shifts in the phase boundaries. The crystallization paths then lead to a relative enrichment of these constituents in the melt. It is suggested here that it is principally this effect which distinguishes the calc-alkali and gabbroic trends of differentiation.

It should be mentioned here that Yoder and Tilley (Reference 45) called upon essentially this mechanism to explain anorthositic magmas as derived from partial melting of amphibolites. In the presence of Ca-amphiboles with higher liquidus temperatures than plagioclase, there will be a tendency for the melt to become enriched in albite. Presumably such partial melting could also give rise to members of the calc-alkali series by subsequent fractional crystallization of the anatectic melt. However, we have seen (Tables 1, 2, and 3) that, in at least some of the large calc-alkali complexes, amphibolitic gabbros are early cumulates or equivalents of parent magmas of the series.

Contrary to the conclusions arrived at here, Best and Mercy (Reference 21) attribute the reducing tendency in the calc-alkali series to volatiles other than H_2 and H_2O . This is surely a misunderstanding, since we have seen that the oxidation state is uniquely defined by the ratios a_{H_2O}/a_{H_2} regardless of the presence of other constituents. However, these other constituents are related to O_2 by their own reactions and must agree with the oxidation state implied by a_{H_2O}/a_{H_2} under equilibrium conditions. Also these authors emphasize the effect of hornblende and biotite on iron enrichment. Although it can be shown that the crystallization of hydrous minerals will tend to decrease a_{H_2O}/a_{H_2} , their appearance is probably more of a symptom of hydrous conditions than a controlling factor in oxidation.

CORRELATIONS AND GENERAL CONCLUSIONS

The systematic variations in the mineral chemistry of the calc-alkali series rocks and the meaning of these correlations in terms of the degree of oxidation and hydration have important implications with respect to the origin of the series.

One of the most important questions which arises is whether the series results from crystallization differentiation or through some other mechanism such as magma mixing, assimilation of cognate inclusions or country rock, or partial fusion of crustal or subcrustal rocks. It has been pointed out by numerous observers that, as we have seen, the quantity of gabbro and other basic rocks in calc-alkali and analogous alkaline complexes is generally small when compared to that of acid or intermediate rocks. Since it is well known that a large volume of basaltic magma is required to produce the late differentiates, this fact is usually used as an argument against their origin by crystallization-differentiation of a basaltic magma. Also, as we have seen, screens of metasedimentary or metavolcanic rocks of prebatholithic age are very common within the batholithic plutons, so it might be supposed that opportunity for contamination through assimilation might be very great indeed.

Fortunately from the standpoint of simplicity, neither of the foregoing suppositions turns out to be true. In the first place, it has been pointed out by Chapman and Williams (Reference 22) that the abundances of the various igneous rock types in any area would be a function of the densities of the corresponding magmas. That the same is also true of solid rocks has been stressed by Ramberg (Reference 48). He has concluded, through scaled experimental models and theoretical arguments, that solid granitic plutons should rise like salt domes through denser crustal rock and that the associated structures are similar to those frequently encountered in the vicinity of batholithic plutons. Thus it seems clear that, although vast volumes of gabbroic or basaltic magmas may be involved in the production of the calc-alkali batholiths, little or no sign of this relationship may appear in the upper levels which are ultimately exposed by uplift and erosion. Consequently there is no necessary relation between the volume of gabbroic rocks exposed and the differentiation history of the batholith.

Similarly, when we consider the possible contamination of the batholithic magmas through assimilation of country rocks, we find that the evidence is largely negative. Although, as was noted by Nockolds (Reference 20) for the Garabal Hill-Glen Fyne complex, such contamination may be apparent locally, it is seldom sufficient to have an important effect on the chemistry. That the quantity of assimilation was minor for the southern California batholith is strongly indicated by the chemistry of the San Marcos gabbro. Although these gabbros are characteristically intrusive into pelitic country rocks, we have seen (Table 1) that they are in fact lower in K_2O than the average tholeiitic basalt. And this is true in spite of the fact that the high-temperature hydrous magmas that they represent should have been, of all members of the series, the most capable of assimilating country rocks. Unfortunately, this criterion cannot be easily applied to rocks later in the series, since these have high K_2O contents by virtue of the differentiation process. However, Larsen's (Reference 8) variation diagrams show that a relatively low K_2O trend characterizes all the rocks of the southern California batholith. Also, calc-alkali series rocks seldom show a marked enrichment of Al_2O_3 in late members of the subsequence; if this showing did occur, we should expect to find cordierite- or sillimanite-bearing granites to be quite common.

When we consider the possibility of deriving the calc-alkali series by the assumption of basic cognate inclusions by granite magmas, we also encounter difficulties. Although the reactions

involved may be exothermic, much liquid is consumed in the process (Reference 49). Moreover, the products of such a process should lie on straight-line variation diagrams quite unlike Figures 1 and 4.

Contamination or partial fusion of crustal rocks to yield the observed series would also have to account for such systematic variations in $\log P_{O_2}$ as are implied by Figure 2. But we have, in fact, little reason to believe that such rocks would be of constant or systematically varying oxidation state. Even less likely would be the near-duplication in widely separated regions of the patterns represented by Figures 1 and 4.

We therefore conclude that the chemical evidence is greatly in favor of an origin of the calc-alkali series by crystallization differentiation of a basaltic or more basic magma and that such differentiation occurs chiefly at depths at which the common crustal rock-forming minerals such as feldspar, pyroxene, and olivine are stable. The data of Yoder and Tilley (Reference 45) on the upper stability limits of hornblendes indicate that the amphibolitic gabbros probably crystallized at water pressures of 2,000 bars or more, and it seems likely that water pressures in the late differentiates were even greater.

It has been suggested (Reference 50) and shown to be theoretically feasible (Reference 15) that successively more siliceous magmas can be derived by partial fusion of a high-pressure assemblage consisting of garnet and pyroxene. Recently experimental evidence which appears to confirm this theory was invoked by Green and Ringwood (Reference 51) to derive the calc-alkali series by partial fusion of quartz eclogite. It is beyond the scope of the present paper to evaluate these results, and it is not the intention of the writer to deny that some members of the calc-alkali series might at times have originated through such deep-seated anatexis. However, in the group of rocks examined—and these represent some of the most extensive calc-alkali complexes known—there is ample evidence for crystallization differentiation of a basaltic magma.

ACKNOWLEDGMENTS

The writer gratefully acknowledges the National Science Foundation, which in part supported this work through grant GA-307. He is also grateful for discussions with Dr. L. S. Walter of Goddard Space Flight Center and to Dr. D. H. Lindsley for his comments.

Goddard Space Flight Center
National Aeronautics and Space Administration
Greenbelt, Maryland, December 26, 1968
188-45-01-01-51

REFERENCES

1. Wager, L. R., and Deer, W. A., "Geological Investigations in East Greenland—Part III. The Petrology of the Skaergaard Intrusion Kangerdlugssuag, East Greenland," *Medd. om Grønland*, 105, pp. 1-352, 1939.

2. Bowen, N. L., Schairer, J. F., and Willems, H. W. V., "The Ternary System: Na_2SiO_3 – Fe_2O_3 – SiO_2 ," *American Journal of Science*, Fifth Series, pp. 405–455, December 1930.
3. Fenner, C. N., "The Crystallization of Basalts," *American Journal of Science*, Fifth Series, 18, pp. 225–253, September 1929.
4. Osborn, E. F., "Role of Oxygen Pressure in the Crystallization and Differentiation of Basaltic Magma," *American Journal of Science*, 257, pp. 609–647, November 1959.
5. Kennedy, G. C., "Equilibrium between Volatiles and Iron Oxides in Igneous Rocks," *American Journal of Science*, 246, pp. 529–549, September 1948.
6. Kennedy, G. C., "Some Aspects of the Role of Water in Rock Melts," *Geological Society of America Special Paper 62, Crust of the Earth*, pp. 489–503, 1955.
7. Muan, A., and Osborn, E. F., "Phase Equilibria at Liquidus Temperatures in the System MgO – FeO – Fe_2O_3 – SiO_2 ," *Journal of the American Ceramic Society*, 39, pp. 121–140, April 1956.
8. Larsen, E. S., Jr., "Batholith and Associated Rocks of Corona, Elsinore, and San Luis Rey Quadrangles, Southern California," *Geological Society of America Memoir 29*, 1948.
9. Mueller, R. F., and Condie, K. C., "Stability Relations of Carbon Mineral Assemblages in the Southern California Batholith," *Journal of Geology*, 72, pp. 400–411, July 1964.
10. Hurlbut, C. S., Jr., "Dark Inclusions in a Tonalite of Southern California," *American Mineralogist*, 20, pp. 609–630, September 1935.
11. Miller, F. S., "Petrology of the San Marcos Gabbro, Southern California," *Bulletin of the Geological Society of America*, 48, pp. 1397–1426, October 1937.
12. Nockolds, S. R., and Allen, R., "The Geochemistry of Some Igneous Rock Series," *Geochimica et Cosmochimica Acta*, 4, pp. 105–142, 1953.
13. Hess, H. H., "Stillwater Igneous Complex, Montana," *Geological Society of America Memoir 80*, 1960.
14. Larsen, E. S., Jr., and Draisin, W. M., "Composition of the Minerals in the Rocks of the Southern California Batholith," *International Geological Congress Report 18th Session Great Britain*, pt. 2, pp. 66–79, 1948.
15. Mueller, R. F., "Interaction of Chemistry and Mechanics in Magmatism," *Journal of Geology*, 71, pp. 759–772, November 1963.
16. Hietanen, Anna, "Metamorphism of the Belt Series in the Elk River–Clarkia Area, Idaho," *U. S. Geological Survey Professional Paper 344-C*, 1963.

17. Hietanen, Anna, 'Idaho Batholith near Pierce and Bungalo, Clearwater County, Idaho," U. S. Geological Survey Professional Paper 344-D, 1963.
18. Bateman, P. C., Clark, L. D., Huber, N. K., Moore, J. G., and Rinehart, C. D., "The Sierra Nevada Batholith—a Synthesis of Recent Work across the Central Part, U. S. Geological Survey Professional Paper 414-D, 1963.
19. Larsen, E. S., Jr., and Schmidt, R. G., "A Reconnaissance of the Idaho Batholith and Comparison with the Southern California Batholith," U. S. Geological Survey Bulletin 1070-A, 1958.
20. Nockolds, S. R., "The Garabal Hill-Glen Fyne Igneous Complex," *Quarterly Journal of the Geological Society of London*, 96, pp. 451-511, 1940.
21. Best, M. G., and Mercy, E. L. P., "Composition and Crystallization of Mafic Minerals in the Guadalupe Igneous Complex, California," *American Mineralogist*, 52, pp. 436-474, March-April 1967.
22. Chapman, R. W., and Williams, C. R., "Evolution of the White Mountain Magma Series," *American Mineralogist*, 20, pp. 502-530, July 1935.
23. Taubeneck, W. H., "Geology of the Elkhorn Mountains, Northeastern Oregon, Bald Mountain Batholith," *Bulletin of the Geological Society of America*, 68, pp. 181-238, February 1957.
24. Johannsen, A., "A Descriptive Petrography of the Igneous Rocks," Chicago, Ill.: University of Chicago Press, 1939.
25. Larsen, E. S., Jr., and Cross, W., "Geology and Petrology of the San Juan Region, Southwestern Colorado," U. S. Geological Survey Professional Paper 258, 1956.
26. Mueller, R. F., "Oxidation in High Temperature Petrogenesis," *American Journal of Science*, 259, pp. 460-480, June 1961.
27. Carmichael, I. S. E., "The Pyroxenes and Olivines from Some Tertiary Acid Glasses," *Journal of Petrology*, 1, pp. 309-336, 1960.
28. Mueller, R. F., "System Fe-MgO-SiO₂-O₂ with Application to Terrestrial Rocks and Meteorites," *Geochimica et Cosmochimica Acta*, 29, pp. 967-976, August 1965.
29. Buddington, A. F., and Lindsley, D. H., "Iron-Titanium Oxide Minerals and Synthetic Equivalents," *Journal of Petrology*, 5, pp. 310-357, June 1964.
30. Mueller, R. F., "Analysis of Relations among Mg, Fe and Mn in Certain Metamorphic Minerals," *Geochimica et Cosmochimica Acta*, 25, pp. 267-296, December 1961.
31. Vincent, E. A., and Phillips, R., "Iron-Titanium Oxide Minerals in Layered Gabbros of the Skaergaard Intrusion, East Greenland," *Geochimica et Cosmochimica Acta*, 6, pp. 1-26, 1954.

32. Robie, R. A., "Thermodynamic Properties of Minerals," in *Handbook of Physical Constants*, ed. by S. P. Clark, Geological Society of America Memoir 97, 1966.
33. Kelley, K. K., "Contributions to the Data on Theoretical Metallurgy XIII. High-temperature Heat-content, Heat-capacity, and Entropy Data for the Elements and Inorganic Compounds," U. S. Bureau of Mines Bulletin 584, 1960.
34. Lindsley, D. H., MacGregor, I. D., and Davis, B. T. C., "Synthesis and Stability of Ferrosilite," *Annual Report of the Director of the Geophysical Laboratory, 1963-1964*, Carnegie Institution of Washington (D. C.), pp. 174-176, 1965.
35. Lindsley, D. H., Speidel, D. H., and Nafziger, R. H., "P-T-f_{O₂} Relations for the System Fe-O-SiO₂," *American Journal of Science*, 266, pp. 342-360, May 1968.
36. Olsen, E. J., and Fuchs, L. H., "The State of Oxidation of Some Iron Meteorites," *Icarus*, 6, pp. 242-253, 1967.
37. Rossini, F. D., Pitzer, K. S., Taylor, W. J., Ebert, J. P., Kilpatrick, J. E., Becket, C. W., Williams, M. G., and Werner, H. G., "Selected Values of Properties of Hydrocarbons," National Bureau of Standards Circular C-461, 1947.
38. Nordlie, B. E., "The Composition of the Basaltic Gas Phase," Ph. D. thesis, University of Chicago, Chicago, Ill., 1967.
39. Wasserburg, G. J., "The Effects of H₂O in Silicate Systems," *Journal of Geology*, 65, pp. 15-23, January 1957.
40. Shaw, H. R., "Theoretical Solubility of H₂O in Silicate Melts Quasi-crystalline Models," *Journal of Geology*, 72, pp. 601-617, 1964.
41. Goranson, R. W., "Phase Equilibrium in the NaAlSi₃O₈-H₂O and KAlSi₃O₈-H₂O Systems at High Temperatures and Pressures," *Am. Jour. Sci. Ser.*, 5, 35A, p. 71, 1938.
42. Fudali, R. F., "Oxygen Fugacities of Basaltic and Andesitic Magmas," *Geochimica et Cosmochimica Acta*, 29, pp. 1063-1075, September 1965.
43. Tuttle, O. F., and Bowen, N. L., "Origin of Granite in the Light of Experimental Studies in the System NaAlSi₃O₈-KAlSi₃O₈-SiO₂-H₂O," Geological Society of America Memoir 74, 1958.
44. Yoder, H. S., Stewart, D. B., and Smith, J. R., "Ternary Feldspars," *Annual Report of the Director of the Geophysical Laboratory, 1956-1957*, Carnegie Institution of Washington (D. C.), pp. 206-214, 1958.
45. Yoder, H. S., and Tilley, C. E., "Origin of Basalt Magmas: An Experimental Study of Natural and Synthetic Rock Systems," *Journal of Petrology*, 3, pp. 342-532, 1962.

46. Clark, S. P., "High Pressure Phase Equilibria," in *Handbook of Physical Constants*, Geological Society of America Memoir 97, 1966.
47. Lindsley, D. H., and Emslie, R. F., "Effect of Pressure on the Boundary Curve in the System Diopside-Albite-Anorthite," *Annual Report of the Director of the Geophysical Laboratory, 1966-1967*, Carnegie Institution of Washington (D. C.), pp. 479-480, 1968.
48. Ramberg, Hans, "Gravity, Deformation and the Earth's Crust," New York: Academic Press, 1967.
49. Bowen, N. L., "The Evolution of Igneous Rocks," Princeton, N. J.: Princeton University Press, 1928.
50. Larsen, E. S., Jr., "Petrographic Province of Central Montana," *Bulletin of the Geological Society of America*, 51, pp. 887-948, June 1940.
51. Green, T. H., and Ringwood, A. E., "Origin of the Calc-alkaline Igneous Rock Suite," *Earth and Planetary Science Letters*, 1, pp. 307-316, September 1966.

NATIONAL AERONAUTICS AND SPACE ADMINISTRATION
WASHINGTON, D. C. 20546
OFFICIAL BUSINESS

FIRST CLASS MAIL



POSTAGE AND FEES PAID
NATIONAL AERONAUTICS AND
SPACE ADMINISTRATION

010 001 31 51 305 69286 00903
AIR FORCE WEAPONS LABORATORY/WLIL/
Kirtland Air Force Base, New Mexico 8711

WILLIAM E. LOUGHEED, CHIEF, TECH. LIBRARY

POSTMASTER: If Undeliverable (Section 158
Postal Manual) Do Not Return

"The aeronautical and space activities of the United States shall be conducted so as to contribute . . . to the expansion of human knowledge of phenomena in the atmosphere and space. The Administration shall provide for the widest practicable and appropriate dissemination of information concerning its activities and the results thereof."

—NATIONAL AERONAUTICS AND SPACE ACT OF 1958

NASA SCIENTIFIC AND TECHNICAL PUBLICATIONS

TECHNICAL REPORTS: Scientific and technical information considered important, complete, and a lasting contribution to existing knowledge.

TECHNICAL NOTES: Information less broad in scope but nevertheless of importance as a contribution to existing knowledge.

TECHNICAL MEMORANDUMS: Information receiving limited distribution because of preliminary data, security classification, or other reasons.

CONTRACTOR REPORTS: Scientific and technical information generated under a NASA contract or grant and considered an important contribution to existing knowledge.

TECHNICAL TRANSLATIONS: Information published in a foreign language considered to merit NASA distribution in English.

SPECIAL PUBLICATIONS: Information derived from or of value to NASA activities. Publications include conference proceedings, monographs, data compilations, handbooks, sourcebooks, and special bibliographies.

TECHNOLOGY UTILIZATION PUBLICATIONS: Information on technology used by NASA that may be of particular interest in commercial and other non-aerospace applications. Publications include Tech Briefs, Technology Utilization Reports and Notes, and Technology Surveys.

Details on the availability of these publications may be obtained from:

SCIENTIFIC AND TECHNICAL INFORMATION DIVISION
NATIONAL AERONAUTICS AND SPACE ADMINISTRATION
Washington, D.C. 20546